

Prediction of phase transition in CaSiO₃ perovskite and implications for lower mantle structure

LARS STIXRUDE,¹ RONALD E. COHEN,² RICI YU,³ AND HENRY KRAKAUER³

¹Department of Earth and Atmospheric Sciences, Georgia Institute of Technology, Atlanta GA 30332-0340

²Geophysical Laboratory and Center for High Pressure Research, Carnegie Institution of Washington, 5251 Broad Branch Rd., N.W., Washington, DC 20015-1305

³Department of Physics, College of William and Mary, Williamsburg, VA 23187-8795

ABSTRACT

First-principles linear-response calculations were used to investigate the lattice dynamics of what is thought to be the third most abundant phase in the lower mantle, CaSiO₃ perovskite. The commonly assumed cubic structure (*Pm3m*) was found to be dynamically unstable at all pressures, exhibiting unstable modes along the Brillouin zone edge from the M point to the R point. On the basis of these results, we predict that the ground-state structure of CaSiO₃ perovskite is a distorted phase with lower than cubic symmetry. We predict that a phase transition occurs in CaSiO₃ perovskite within the Earth's lower mantle from the low-temperature distorted phase to the high-temperature cubic phase. The predicted phase transition possibly explains some of the seismological observations of reflective features within the lower mantle.

INTRODUCTION

CaSiO₃ perovskite is thought to comprise between 6 and 12 wt% of the lower half of the Earth's transition zone and lower mantle (depths between 500 and 2900 km) (Irifune 1994; O'Neill and Jeanloz 1990; Ita and Stixrude 1992). Its structure throughout this regime is generally assumed to be cubic because X-ray diffraction studies have found no detectable deviation from *Pm3m* symmetry (Liu and Ringwood 1975; Mao et al. 1989; Wang et al. 1996). Theoretical studies based on ionic models (Wolf and Jeanloz 1985; Hemley et al. 1987; Wolf and Bukowinski 1992), periodic Hartree-Fock calculations (Sherman 1993), and pseudopotential calculations (Wentzcovitch et al. 1995) have supported this view.

In the present paper, we go beyond previous studies by investigating from first principles the full phonon spectrum of cubic CaSiO₃ perovskite from low pressures to those typical of the lower mantle. The calculations are based on the linearized augmented plane-wave (LAPW) method, widely accepted as among the most accurate methods for solving the band structure and total energy problem. We found that the cubic phase is dynamically unstable at all pressures and that the ground-state structure must have lower than cubic symmetry.

These results are important for our understanding of the physics and chemistry of this mantle phase; its phase stability, elasticity, and ability to incorporate other cations such as Mg, Fe, and Al, for example, are affected by its symmetry. Moreover, the existence of a low-symmetry ground state raises the possibility of a temperature-induced phase transition in this mineral within the Earth. Phase transitions in lower mantle constituents have important implications for our understanding of recent seis-

mological observations of reflective features within the lower mantle (Revenaugh and Jordan 1991; Kawakatsu and Niu 1994; LeStunff et al. 1995) near 700, 900, and 1200 km depth. These observations indicate the presence of previously unpredicted phase transitions or sharply bounded compositional heterogeneities, challenging our traditional view of this region as being compositionally and mineralogically homogeneous.

COMPUTATIONS

The LAPW linear-response calculations determined the self-consistent first-order response of the electronic charge density to generalized perturbations (Yu and Krakauer 1994). The calculations are based on density functional theory; the only essential approximation is the exchange-correlation potential. We used the well-studied local density approximation (LDA), which has been applied successfully in studies of silicates, including MgSiO₃ perovskite (Stixrude and Cohen 1993). We computed the linear response to shifts in nuclear positions and imposed external fields, which yielded the elements of the dynamical matrix, the dielectric constant (ϵ), and the Born effective charges (Z^*), from which the phonon frequencies were determined (Yu and Krakauer 1995; Lee and Gonze 1994). The perturbations need not be commensurate with the unit cell, so points in the Brillouin zone away from the zone center were readily investigated. We calculated the dynamical matrix of the cubic *Pm3m* phase of CaSiO₃ perovskite at four points in the Brillouin zone (Γ , X, M, R). Computational variables (k -point mesh: $4 \times 4 \times 4$ for computations of the dynamical matrix elements, $8 \times 8 \times 8$ for ϵ and Z^* ; number of basis functions per atom ≈ 150) were chosen such that phonon frequencies con-

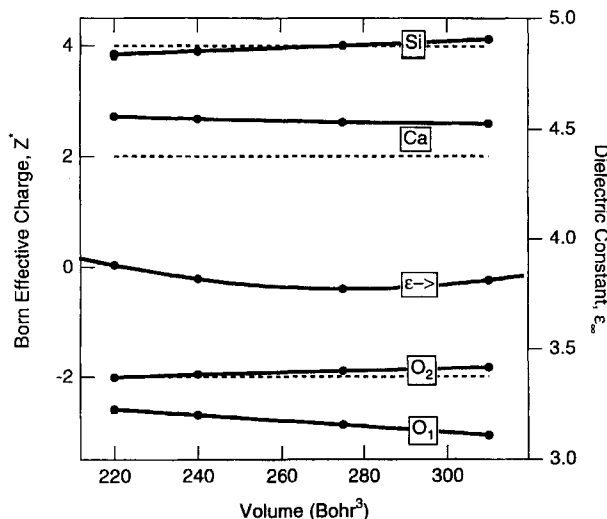


FIGURE 1. Born effective charges (left axis) and dielectric constant (right axis) as a function of compression. Pressures range from -8 GPa ($V = 310$ bohr³) to 140 GPa ($V = 220$ bohr³) and were determined by fitting a third-order finite strain expression to the LAPW total energy as a function of volume. The two symmetrically distinct elements of the O Born effective charge tensor are shown, Z_{O_1} for motion of O along the Si-O bond, and Z_{O_2} for motion normal to the bond. Dashed lines indicate formal ionic charges.

verged to better than one wavenumber. The full phonon-dispersion curve was determined using an interpolation scheme that separates short-range forces from long-range, coulombic interactions (Yu and Krakauer 1994; Gonze et al. 1994).

RESULTS

We found that the Born effective charges in CaSiO₃ perovskite differ significantly from formal ionic charges, by as much as $1e$ (Fig. 1). Compression causes Z^* of Si and Ca to deviate farther from their formal ionic values, and Z^* of O to approach -2 . The dielectric constant, $\epsilon = 3.8$ at zero pressure, lies between the known values for CaO (Lide and Frederikse 1994) and SiO₂ stishovite (Stishov and Popova 1961) and varies slowly with pressure (Fig. 1). LO-TO splitting of zone-center vibrational frequencies is on the order of 50 – 200 wavenumbers (Fig. 2). All zone-center modes were found to be dynamically stable. Examination of the eigenvectors showed that the highest frequency modes involve stretching of the octahedral Si-O bond. The change in frequency of these modes with compression is greatest because the length of the Si-O bond shrinks in direct proportion to compression in the cubic structure.

The full phonon-dispersion curves reveal dynamical instabilities in the cubic structure along the zone boundaries (Fig. 2). Instabilities occur at the M and R points and along the zone edges from M to R. The corresponding imaginary frequencies grow in magnitude with compression. Examination of the eigenvectors associated with

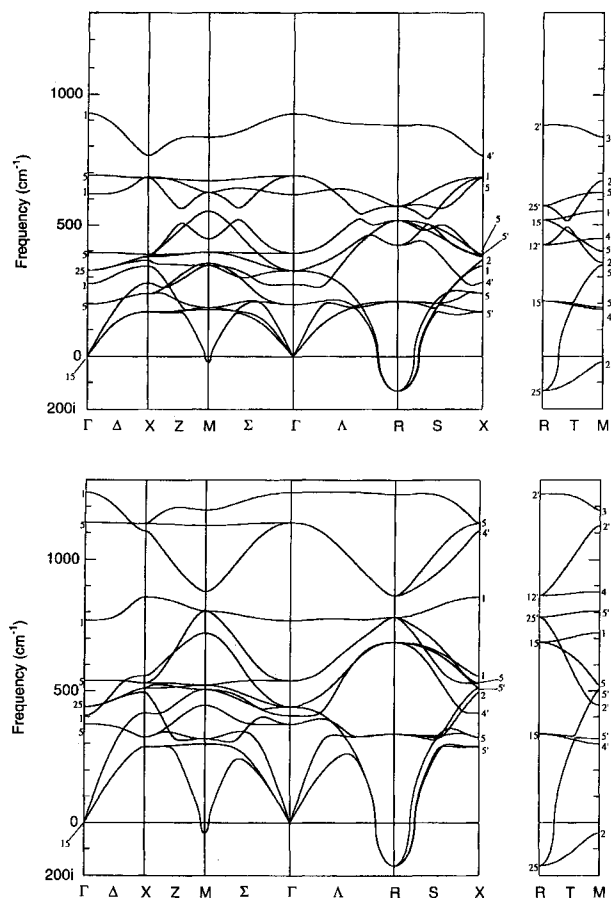


FIGURE 2. Phonon spectrum of the cubic phase at $V = 310$ bohr³ ($P = -8$ GPa) (top) in comparison with that at $V = 240$ bohr³ ($P = 80$ GPa) (bottom). All zone-center modes (Γ point) are stable, as shown by the existence of imaginary frequencies. The final panel (M-R) shows that the edges of the cubic Brillouin zone are unstable throughout. The magnitude of the imaginary eigenfrequencies increases with compression. Symmetry designations are those of Cowley (1964) as corrected by Boyer and Hardy (1981). At Γ there are four TO modes (Γ_3 and inactive Γ_{25} symmetries) and three LO modes (Γ_1). The volume dependence of the zone-center modes is described by $\omega = \omega_0(V_0/V)^\gamma$, where the frequencies at $V = 310$ bohr³ (near-zero pressure), $\omega = \omega_0$, are 197 , 274 , 327 , 393 , 621 , 691 , and 926 cm⁻¹; and the respective mode Grüneisen parameters, γ_i , are 2.5 , 1.5 , 1.2 , 1.2 , 0.8 , 2.0 , and 1.2 .

these unstable modes showed that they consist of coupled rotations of the SiO₆ octahedra. The unstable modes at the M point (M_2) and R point (R_{25}) are associated, respectively, with in-phase and out-of-phase rotations of the octahedra about $[100]$. Instabilities along M-R were previously found in ionic model calculations but only at pressures (P) above 80 GPa (Hemley et al. 1987; Wolf and Bukowinski 1992). Here we found that the instabilities are more profound and that they persist even in the expanded lattice ($P = -8$ GPa). Unstable modes of the

same type have also been found in theoretical investigations of cubic MgSiO₃ perovskite, which account for the observed orthorhombic (*Pbnm*) symmetry of this material (Wolf and Jeanloz 1985; Hemley et al. 1987; Wolf and Bukowinski 1992).

Our results indicate that the cubic *Pm3m* structure of CaSiO₃ perovskite is dynamically unstable and that the ground state of this material must have lower symmetry. However, the ground state is not of direct relevance to the lower mantle, where temperatures exceed 2000 K. Even if the cubic phase is dynamically unstable, it may be thermodynamically stable at high temperatures because of its greater entropy (e.g., Salje 1990).

The temperature at which the low-temperature distorted phase transforms to the high-temperature cubic phase depends not only on the unstable mode frequencies but also on the energetics of finite displacements along the unstable mode eigenvectors. Using LAPW total energy calculations, we found the total energy as a function of displacement along the most unstable mode eigenvector (R_{25}) and the associated minimum-energy displacement (frozen phonon approach; Cohen 1992). The symmetry of the structure associated with this finite displacement is tetragonal *I4/mcm*, with ten atoms in the unit cell. The results at midmantle pressures ($P = 80$ GPa) show that the minimum-energy displacement corresponds to an octahedral rotation angle of 7° and is 360 K per octahedron lower in energy than the cubic phase (Fig. 3). The relatively small minimum-energy octahedral rotation angle may explain why previous X-ray diffraction experiments have failed to detect deviations from cubic symmetry. With the assumption that the octahedral rotations are rigid (O'Keefe et al. 1979), the corresponding c/a ratio of the distorted phase differs by only 0.7% from that of the cubic structure, which is below the detection limit of previous nonhydrostatic (Mao et al. 1989) and quasi-hydrostatic (Wang et al. 1996) experiments (H.K. Mao, personal communication).

These results constrained the parameters of a simple model that we used to estimate the transition temperature from the distorted *I4/mcm* structure to the cubic *Pm3m* structure. The model (Bruce 1980) consists of on-site terms, which correspond to finite displacements along the unstable zone-boundary mode eigenvectors, and intersite couplings

$$U = \sum_i V(Q_i) + \frac{J}{2} \sum_{i,j}^m (Q_i + Q_j)^2 \quad (1)$$

where U is the energy contained in octahedral rotations, Q is the normal coordinate of the octahedral rotation, and $V(Q)$ is the on-site term given by our total energy results (Fig. 3). The form of the nearest-neighbor intersite coupling term is determined by the requirement that it vanish for a pure R_{25} mode distortion of the crystal, in which neighboring octahedra rotate in opposite directions. The intersite coupling parameter, J , is most simply given by the curvature along Γ -R of the unstable mode

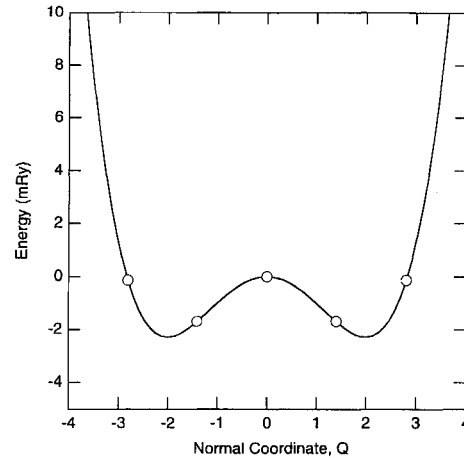


FIGURE 3. Total energy (per octahedron) of the *I4/mcm* tetragonal structure as a function of finite displacement along the R_{25} eigenvector at $V = 240$ bohr³ ($P = 80$ GPa). The LAPW total energy results (symbols) were fitted to a polynomial of the square of the normal coordinate, Q : $V(Q) = A Q^2/2 + B Q^4/4$. The normal coordinate per octahedron, $Q^2 = \frac{1}{2} \sum_i^n m_i x_i^2$, where the sum is over the cartesian displacements (x_i , in bohr) of the n atoms in the unit cell, with masses, m_i , in atomic mass units. This expression, with $A = -2.04$ mRy amu⁻¹ bohr⁻² and $B = 0.456$ mRy amu⁻¹ bohr⁻⁴, constrains the on-site term in the simple model of the phase transition discussed in the text. The remaining parameter, $J = 1.19$ mRy amu⁻¹ bohr⁻², is determined from the dispersion of the unstable mode eigenvalue (Fig. 2). The unstable mode frequency in the cubic phase ($Q = 0$) calculated from the curvature of the polynomial fit (173i cm⁻¹, $i = \sqrt{-1}$) agrees with the linear-response result (164i cm⁻¹).

eigenenergy evaluated at the R point (Fig. 2). The relative magnitudes of the on-site and intersite coupling terms are such that the phase transition is expected to occur in the displacive limit. In this case, if we ignore coupling between the unstable mode eigenvector and other modes, the transition temperature is given by

$$T_c = \frac{4}{3q(3)} \frac{J|A|}{k_B B} \approx 2200 \text{ K} \quad (2)$$

where k_B is the Boltzmann constant and $q(3) = 0.5054$. The estimated transition temperature is similar to estimates of temperatures in the lower mantle at similar pressures: $P = 80$ GPa corresponds to a depth of 1850 km and a temperature of approximately 2500–3000 K.

DISCUSSION

Our estimate of T_c may be uncertain by several hundred kelvins and is likely to be a lower limit because we have ignored coupling between unstable mode eigenvectors, which may lower the total energy of the distorted phase further relative to the cubic phase. Nevertheless, the fact that our estimated T_c is comparable to lower mantle temperatures indicates that a phase transition in CaSiO₃ perovskite is likely to occur in the lower mantle.

The predicted phase transition in CaSiO₃ perovskite is expected to be associated with an elastic anomaly, which may be the cause of at least a subset of the reflective features near 700, 900, and 1200 km depth in the lower mantle (Revenaugh and Jordan 1991; Kawakatsu and Niu 1994; LeStunff et al. 1995). Other phase transitions have been discussed as possibly occurring in the Earth's lower mantle. A phase transition in the lower mantle's most abundant constituent, MgSiO₃ perovskite, has been suggested (Meade et al. 1995), but theoretical computations show such a transition unlikely for reasonable geotherms (Stixrude and Cohen 1993; Warren and Ackland 1996). Recent results have shown that SiO₂ undergoes a phase transition from the stishovite to the CaCl₂ structure at lower mantle pressures (Cohen 1992; Kingma et al. 1995). Our results on CaSiO₃ perovskite indicate the presence of yet another phase transition within the lower mantle, the first high-pressure phase transition predicted with the linear-response method.

ACKNOWLEDGMENTS

We thank H.K. Mao and R.J. Hemley for helpful discussions. This work was supported by NSF under grants EAR-9305060 (L.S.), EAR-9304624 (R.E.C.), EAR-9418934 (R.E.C.), and DMR-9404954 (H.K.). Calculations were performed on the Cray C90 at the Pittsburgh Supercomputer Center and the Cray J90 at the Geophysical Laboratory.

REFERENCES CITED

- Boyer, L.L., and Hardy, J.R. (1981) Theoretical study of the structural phase transition in RbCaF₃. *Physical Review B*, 24, 2577–2591.
- Bruce, A.D. (1980) Structural phase transitions: II. Static critical behaviour. *Advances in Physics*, 29, 111–217.
- Cohen, R.E. (1992) First-principles predictions of elasticity and phase transitions in high pressure SiO₂ and geophysical implications. In Y. Syono and M.H. Manghni, Eds., *High pressure research: Applications to earth and planetary sciences*, p. 425–432. American Geophysical Union, Washington, D.C., and Terra Scientific, Tokyo.
- Cowley, R.A. (1964) Lattice dynamics and phase transitions of strontium titanate. *Physical Review*, 134, A981–A997.
- Gonze, X., Charlier, J.-C., Allan, D.C., and Teter, M.P. (1994) Interatomic force constants from first principles: The case of alpha-quartz. *Physical Review B*, 50, 13035–13038.
- Hemley, R.J., Jackson, M.D., and Gordon, R.G. (1987) Theoretical study of the structure, lattice dynamics, and equations of state of perovskite-type MgSiO₃ and CaSiO₃. *Physics and Chemistry of Minerals*, 14, 2–12.
- Irifune, T. (1994) Absence of an aluminous phase in the upper part of the earth's lower mantle. *Nature*, 370, 131–133.
- Ita, J.J., and Stixrude, L. (1992) Petrology, elasticity, and composition of the mantle transition zone. *Journal of Geophysical Research*, 97, 6849–6866.
- Kawakatsu, H., and Niu, F.L. (1994) Seismic evidence for a 920-km discontinuity in the mantle. *Nature*, 371, 301–305.
- Kingma, K.J., Cohen, R.E., Hemley, R.J., and Mao, H.K. (1995) Transformation of stishovite to a denser phase at lower-mantle pressures. *Nature*, 374, 243–245.
- Lee, C., and Gonze, X. (1994) Lattice dynamics and dielectric properties of SiO₂ stishovite. *Physical Review Letters*, 72, 1686–1689.
- LeStunff, Y., Wicks, C.W., and Romanowicz, B. (1995) P'P' precursors under Africa: Evidence for mid-mantle reflectors. *Science*, 270, 74–77.
- Lide, D.R., and Frederikse, H.P.R., Eds. (1994) *CRC handbook of chemistry and physics*, 75e. CRC Press, Boca Raton.
- Liu, L.-G., and Ringwood, A.E. (1975) Synthesis of a perovskite-type polymorph of CaSiO₃. *Earth and Planetary Science Letters*, 14, 1079–1082.
- Mao, H.K., Chen, L.C., Hemley, R.J., Jephcoat, A.P., Wu, Y., and Bassett, W.A. (1989) Stability and equation of state of CaSiO₃ perovskite to 134 GPa. *Journal of Geophysical Research*, 94, 17889–17894.
- Meade, C., Mao, H.K., and Hu, J.Z. (1995) High-temperature phase transition and dissociation of (Mg,Fe)SiO₃ perovskite at lower mantle pressures. *Science*, 268, 1743–1745.
- O'Keefe, M., Hyde, B.G., and Bovin, J. (1979) Contribution to the crystal chemistry of orthorhombic perovskite: MgSiO₃ and NaMgF₃. *Physics and Chemistry of Minerals*, 4, 299–305.
- O'Neill, B., and Jeanloz, R. (1990) Experimental petrology of the lower mantle: A natural peridotite taken to 54 GPa. *Geophysical Research Letters*, 17, 1477–1480.
- Revenaugh, J., and Jordan, T.H. (1991) Mantle layering from SCS reverberations: 2. the transition zone. *Journal of Geophysical Research*, 96, 19763–19780.
- Salje, E.K.H. (1990) Phase transitions in ferroelastic and co-elastic crystals, 366 p. Cambridge University Press, Cambridge.
- Sherman, D.M. (1993) Equation of state, elastic properties, and stability of CaSiO₃ perovskite: 1st principles (periodic Hartree-Fock) results. *Journal of Geophysical Research*, 98, 19795–19805.
- Stishov, S.M., and Popova, S.V. (1961) New dense polymorphic modification of silica. *Geokhimiya*, 10, 837–847.
- Stixrude, L., and Cohen, R.E. (1993) Stability of orthorhombic MgSiO₃ perovskite in the earth's lower mantle. *Nature*, 364, 613–616.
- Wang, Y., Weidner, D.J., and Guyot, F. (1996) Thermal equation of state of CaSiO₃ perovskite. *Journal of Geophysical Research*, 101, 661–672.
- Warren, M.C., and Ackland, G.J. (1996) Ab initio studies of structural instabilities in magnesium silicate perovskite. *Physics and Chemistry of Minerals*, 23, 107–118.
- Wentzcovitch, R., Ross, N.L., and Price, G.D. (1995) Ab initio study of MgSiO₃ and CaSiO₃ perovskites at lower-mantle pressures. *Physics of the Earth and Planetary Interiors*, 90, 101–112.
- Wolf, G.H., and Jeanloz, R. (1985) Lattice dynamics and structural distortions of CaSiO₃ and MgSiO₃ perovskites. *Geophysical Research Letters*, 12, 413–416.
- Wolf, G.H., and Bukowinski, M.S.T. (1992) Theoretical study of the structural properties and equations of state of MgSiO₃ and CaSiO₃ perovskite: Implications for lower mantle composition. In M.H. Manghni and Y. Syono, Eds., *High-Pressure Research in Mineral Physics*, p. 313–331. American Geophysical Union, Washington, D.C., and Terra Scientific, Tokyo.
- Yu, R., and Krakauer, H. (1994) Linear-response calculations within the linearized augmented plane-wave method. *Physical Review B*, 49, 4467–4477.
- (1995) First-principles determination of chain-structure instability in KNbO₃. *Physical Review Letters*, 74, 4067–4070.

MANUSCRIPT RECEIVED JULY 18, 1996

MANUSCRIPT ACCEPTED AUGUST 3, 1996